1995

Windbreak Shelter as a Function of Wind Direction

James R. Brandle
University of Nebraska - Lincoln, jbrandle1@unl.edu

Published in the preprint volume of the NINTH SYMPOSIUM ON METEOROLOGICAL OBSERVATIONS & INSTRUMENTATION, March 27-31, 1995, Charlotte, NC, by the American Meteorological Society, Boston, MA.

P1.27

WINDBREAK SHELTER AS A FUNCTION OF WIND DIRECTION

R.A. Schmidt*, R.L. Jairell[1]
J.R. Brandle[2], E.S. Takle[3], and I.V. Litvina[4]

[1]USDA Forest Service, Laramie, Wyoming
[2]University of Nebraska, Lincoln, Nebraska
[3]Iowa State University, Ames, Iowa
[4]Agrophysical Research Institute, St. Petersburg, Russia

1. INTRODUCTION

Networks of shelterbelts and forested riparian strips protect croplands in many regions of the globe. Substantial economic benefits from these systems motivate continued research to improve them. Much has been done, but uncertainties still hinder predicting microclimate and benefits, given windbreak architecture and climatic variation. The processes are complicated.

Our efforts to extend understanding of single shelterbelts to a windbreak network led us to begin the field experiments reported in this paper. Most studies of windbreak aerodynamics focus on two-dimensional flow perpendicular to a barrier. Within the smaller set reporting results with oblique winds, most barriers were fences. Shelterbelt protection in oblique winds apparently differs from the effect of more two-dimensional fences. Measurements of windbreak shelter in oblique winds were a logical first step in our studies to expand understanding to atmospheric flow over windbreak networks.

The objective of this paper is to report methods and example results of our initial field studies on oblique flow over shelterbelts. Because we expect these studies will continue, the instrumentation is described in detail, for future reference.

Reviews of windbreak aerodynamics (Heisler and DeWalle, 1988), shelter microclimate (McNaughton, 1988), and flow around obstacles (Taylor, 1988), update an earlier review by van Eimern et al. (1964). Seginer (1975) measured the wind reduction by a 50% porous fence in oblique winds, comparing the protection distance with studies summarized by van Eimern et al. (1964). His results and those of others are included in the review by Heisler and DeWalle, (1988, Fig. 13). For fences, the protection distance d_p perpendicular to the barrier decreases more rapidly than cos α, where α is wind angle, measured from perpendicular. For a tree shelterbelt, measurements by Gorshenin (1946, as reported in van Eimern et al., 1964) showed d_p decreased less rapidly than cos α. However, Seginer (1975) showed that the drag force exerted on the fence did follow the cosine of wind angle.

Mulhearn and Bradley (1977) provided visualizations of flow over oblique fences in a wind tunnel, together with mean velocity and turbulence measurements. Their photographs show direction changes in oblique wind through these fences, even near the center, where end effects were minimum.

2. METHODS

The system described here for measuring vertical profiles of temperature and wind speed was initially designed for studies in blizzards (Tabler, 1980). Design conditions included strong winds, wind-driven snow, and operators wearing gloves. During many improvements, for a variety of new studies, field-worthiness and ease of use remained guiding criteria, to reduce operator exposure during relocation and adjustment. This is offered as explanation for any appearance of overdesign.

2.1 System Overview

Three portable 10-m masts support cup anemometers and temperature sensors at ten levels. A data logger at each mast accumulates measurements that are relayed by radio to computers in a mobile van. Sensors added to each mast for the shelterbelt studies provide measures of wind direction, humidity and radiation. An additional data logger monitors pressure transducers to determine static pressure distributions at the ground near the barrier. Sonic anemometers are added when turbulence data is required.

When the wind is "right", one mast remains at a reference location, while we moved the others to locations of interest, usually along a transect perpendicular to the barrier. Runs of 5-min duration are accumulated continuously, and the observer notes times when the masts are in position and data is valid. Two operators can usually move one mast between

*Corresponding author address: R. A. Schmidt, USDA Forest Service, Rocky Mountain Forest and Range Experiment Station, 222 S. 22nd Street, Laramie, WY, USA. Phone (307) 742-6621 Fax (307) 742-0397

locations and re-level within a 5-min period. Each mast-logger system can be moved by one person, but disconnection may require 10 to 15 min per move.

The radio links allow close synchronization of data loggers, monitoring for system checkout, and real-time testing of hypotheses. The mobile van provides shelter for the observers and transports the entire system.

The remainder of this section provides details of the various subsystems and components.

2.2 Instrument Masts

Built from aluminum, each mast is a 2-section telescoping tube supported at the intersection of a "T"-shaped base, and held vertical by three adjustable braces that extend from the ends of the base to the mid-point of the tube (Fig. 1). The lower tube is 4.9 cm outside diameter, the upper tube, 4.2 cm. Design, construction, and testing details are provided by Jairell et al. (1984). Normal orientation is with the top of the "T" toward the wind. The support tube and side braces pivot at their attachment with the base. Disconnecting the downwind brace from the base channel allows the vertical tube to be lowered for sensor adjustments. A temporary swinging brace clamps to the mast tube for safety during this operation. Crossed levels held to the mast by Velcro* straps speed readjustment to vertical after moving.

The braces disconnect from the base and fold together with the mast tube for transport on the side of the van. Base members disconnect and are carried in a rack on the van's roof.

FIG. 1. Each portable 10-m mast supports ten levels of temperature and wind speed sensors. In addition, wind direction, humidity, and radiation data are accumulated by a solar-powered data logger on the hand cart. This mast is set for wind from the right.

Wheels or skis at the ends of the base facilitate movement in the field. The 25-cm-diameter wheels attach by cantilevered arms (not as in Fig. 1), so the base can be lowered in place, to reduce obstruction of flow near the surface.

For quick adjustments, Vise-grips* secure sensor support arms to the mast tube. The lowest seven arms are joined in a rack, with 25-cm spacing. This feature is important for resetting lowest sensor heights in drifting snow with migrating dunes. Marks at 1-m increments on the mast tube speed positioning sensors.

Sensors attach to the support arm by waterproof bayonet-lock connectors (Fig. 2). Similar connectors near the Vise-grip* mate with a harness of Teflon*-insulated cable that is held to the mast with Velcro* straps (in place of tape). Distance from the center of the anemometer to the outside of the mast tube is 67 cm. The temperature sensor connects to the arm at 37 cm from the mast.

2.2 Anemometers

The cup anemometers, manufactured from Lexan* plastic by Maximum Inc.* (model 40), produce an alternating current with frequency proportional to wind speed. Three conical cups, 5 cm in diameter, are molded in a rotor that sweeps a 19-cm outside diameter (Fig. 2). The distance constant given by the manufacturer is 3 m. Sensors are numbered, and location of each sensor is recorded during setup.

During periodic matching, we run ten sensors at a time at the same height above short-grass at a plains site. This procedure detects problem sensors and provides a correction when highest accuracy is required. Comparison with a propeller-vane (R.M. Young* model 05701) shows the cup anemometer threshold speeds (near 0.5 m s^{-1}) and corrections for overshoot. Bernstein (1966) and Hetzler et al. (1967) consider other errors in using cup anemometers for profile measurements.

2.3 Temperature Sensors

Thermistor networks, a composite two-thermistor bead with two external resistors (Yellow Springs Instruments* model 44203), provide air temperature signals. The network is designed to provide a voltage or resistance that is a linear function of temperature. Each sensor is built on a connector to mate with the connector on the support arm. Potting compound seals the resistors and solder cups, leaving only the bead and a support wire exposed. A plastic pipe "T"

*The use of trade and company names is for the benefit of the reader; such use does not constitute an official endorsement or approval of any service or product by the authors institutions, to the exclusion of others that may be suitable.

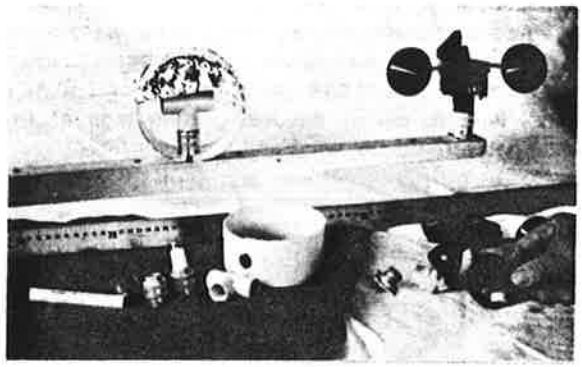

FIG. 2. Waterproof connectors attach the thermistor networks and cup anemometers to the support arms that clamp to the mast. Plastic pipe "T"'s and larger plastic bands provide radiation shielding adequate for the windy conditions of interest.

provides radiation shielding adequate for winter work at high wind speeds. We use an additional shield (Fig. 2) for summer shelterbelt studies. Each sensor is numbered.

Two corrections improve accuracy of the measured temperatures. The first is the manufacturer's specified deviation from linearity (±0.16°C maximum). Two fifth-order polynomials provide close estimates. For experiments at subfreezing temperatures,

$$Z = 0.12 - 6.28E\text{-}03\,A - 1.079E\text{-}03\,A^2 + 3.05E\text{-}05 * A^3 + 1.188E\text{-}06\,A^4 - 2.7426E\text{-}08\,A^5$$

where Z is the corrected temperature and A is the raw temperature computed by the data logger, using the manufacturers's equation. For warm weather experiments (A > 0°C),

$$Z = 0.122 - 6.77E\text{-}03\,A - 1.60E\text{-}03\,A^2 + 9.87E\text{-}05 * A^3 - 1.47E\text{-}06\,A^4 + 3.08E\text{-}09\,A^5$$

A second correction is the offset that accounts for differences between thermistors and resistors in each network (±0.15°C maximum). Calibrating the sensors in a triple-point water bath determines these values. We calibrate ten sensors at a time, using distilled water and finely ground ice in a stainless-steel, insulated container, with a magnetic stirrer. A quartz-crystal thermometer provides a check that the bath is at triple point. Submerging the thermistor beads and monitoring output voltages with the data logger provides the offsets, after they are steady for a 10-min period. These offset corrections change slowly as the thermistors age, requiring recalibration at intervals of several years unless a sensor is repaired or replaced.

By this procedure, temperature differences along a vertical profile are determined within a few hundredths of a degree Celsius. Radiation errors may be larger.

2.4 Data Loggers

A data acquisition subsystem completes the basic profiling equipment at each mast. For mobility, the logger, with battery and solar panel, is mounted on a hand cart (Fig. 3). In the upper enclosure with the logger (Campbell Scientific Inc.* model CR10) are a backup storage module and VHF radio. A larger enclosure below houses a relay multiplexer (CSI* model AM416) to scan the temperature sensors, and two interval-timer modules (CSI* model SMD-INT8) that measure anemometer output frequency. The lower enclosure provides extra space for additional equipment as needed. In operation, lowering the hand cart reduces wind obstruction (Fig.1). A "T"-handled rod, mounted in a swivel on the cart, provides a quick system ground.

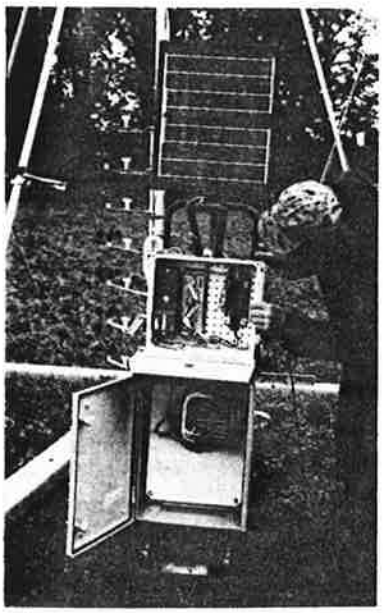

FIG. 3. A solar panel (top) and gel-type automotive battery (bottom) power the data logger and radio in the upper enclosure. During transport, the solar panel folds down over the logger enclosure, and a rucksack strapped to the back of the hand cart stores the cable harness.

2.5 Wind Direction

Propeller-vane sensors (R.M. Young* models 05305 and 05701) provide wind direction and an additional wind speed at each mast. To maintain accurate orientation, the vane is mounted so 180° corresponds to wind directly at the face of the mast. When resetting a mast, the back member of the base is visually alined with field markers on the transect line. True wind direction is computed from the compass

bearing of the transect and the measured vane deviation from 180°.

2.6 Static Pressure at the Surface

Schmidt et al. (1995) present the objective, system design, and initial results of static pressure measurements at the ground, during our studies of wind shelter. The pressure study employs a logger subsystem identical to that in Figure 3, except that three pressure sensors and a 12-port scanning valve replace the electronic modules in the lower enclosure. Two additional hand carts carry racks with eight spools of tubing, to sample pressure along the transect.

2.7 Other Measurements

A humidity sensor (CSI* model 207) in a Gill* radiation shield at 1.5-m height on the back brace of each mast monitors relative humidity. At the same height, a pyranometer (LI-COR* model LI-200SZ) measures hemispheric direct solar and diffuse sky radiation. These data aid interpretation of the primary vertical profile data.

Although not part of these initial experiments, our planned studies require turbulence measurements. We will use several sonic anemometers, as in Figure 1 (Applied Technologies* model BH-478B/3 or more recent versions) to track turbulent structures over the windbreak.

3. STUDY SITE AND SHELTERBELTS

A University of Nebraska research farm was the location for our profile experiments during three periods, in September, 1993, May, and July, 1994. The farm is approximately 50 km northeast of Lincoln, Nebraska, in Saunders County, Township 14 North, Range 8 East, Section 26. Coordinates are 41°09' N, 96°30' W, 343 m elevation. The site is slightly higher, and more nearly level than the moderately rolling surroundings, and provides a variety of shelterbelt arrays. Those used for our initial studies are described below.

3.1 Ash-conifer

These shelterbelt arrays, planted in 1966, have two tree rows, 5 m apart. In each row, trees are spaced at 2.5 m, with alternate species in pairs, two ash, two conifer, etc. Between rows, ash are opposite conifers. The ash (*Fraxinus pennsylvanica*) provided an average maximum height of 12-m, in September, 1993. Conifers, mostly eastern redcedar (*Juniperus virginiana* L.), with some Austrian pine (*Pinus nigra* Arnold), were shorter, increasing foliage in the lower part of the belt.

Optical porosity estimated from night photographs of the shelterbelt back-lit by electronic flash (Fig. 4), averaged 0.26. For eight samples, the 95% confidence interval (CI) was from 0.21 to 0.31. Leaf fall was nearly complete when the photos were taken on 28 September 1993. South winds approached an east-west leg of the array over a fetch of 1-m-high beans, with alfalfa in the lee. Other legs of the shelterbelt array block west and northerly flow.

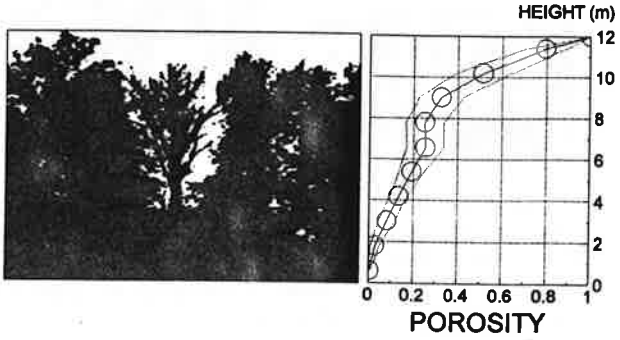

FIG. 4. We photographed the ash-conifer windbreak at night, using an electronic flash fired at several locations behind the barrier, with the camera shutter locked open. Digitized images like the example, left, yielded estimates of optical porosity. The porosity profile at right is an average from 8 slides. Band marks 95% confidence interval.

3.2 Redcedar

The two rows of this eastern redcedar windbreak are 2.5 m apart, with trees at 2.5-m spacing. Planted in 1986, average maximum tree height was 4.75 m at the time of our measurements. Trees in the downwind row are between locations of trees in the upwind row. The belt runs east-west for 460 m, with 6.2 m average distance across the shelterbelt, between branch tips at the base. South winds approached over alfalfa 25 to 35 cm high. The lee was freshly planted, with 10-cm furrows perpendicular to the belt. Optical porosity estimates from digitized daytime photographs (Fig. 5) averaged 0.23 (95% CI, 0.21-0.25).

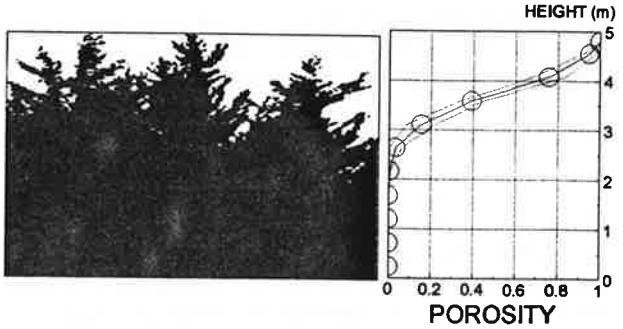

FIG. 5. The example image, left, is digitized from a slide of the redcedar barrier. The optical porosity profile at right is an average from 5 slides, and the band marks the 95% confidence interval. Because optical porosity is zero in the lowest region of this barrier, there was no advantage to night photography.

3.3 Riparian

A wooded riparian strip transects the farm, providing a north-south barrier with 7.3 m average maximum height near our measurement transect. (To measure heights, a distant observer with binoculars reads a survey rod at the belt.) Species include plum (*Prunus americana*), chokecherry (*Prunus virginiana*), willow (*Salix nigra*), and Siberian elm (*Ulmus pumila* L.). The strip was cleared in 1986. Most of the taller trees are rooted in the upper banks, forming a cavity in the foliage, directly above the waterway (Fig. 6). We did not estimate optical porosity of this strip.

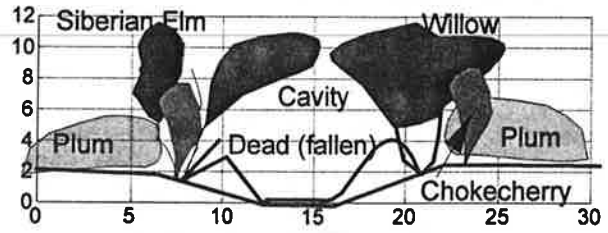

FIG. 6. A cross section through the wooded riparian strip at the transect used for wind profiles in May, 1994, shows the cavity in foliage above the channel. Grid units are meters.

4. EXAMPLE RESULTS

This section compares wind shelter by the redcedar windbreak (Fig. 7), in southwest flow on 10 May with near-perpendicular flow from the south on 13 May, 1994. The measurement transect was 97 m (20.4 *H*) from the west end of the belt. A three-row redcedar barrier runs north from that end. Wind speeds at each level were normalized by 80% of the upwind speed at the same height. Points to the left of the dashed line in Figure 7 represent wind reductions of at least 20%.

The approach wind profiles gave an average roughness parameter, z_0, of 6 cm (H/z_0 = 79) over the alfalfa, with near-neutral to unstable stratification. A period of north wind on 11 May yielded estimates of 0.3 to 0.7 cm for z_0 over the bare planted field that was sheltered on 10 and 13 May. The redeveloping lee profiles clearly show the reduced shelter and speedup near the surface that accompanies the reduction in roughness. Some method of estimating the unsheltered profile *over the same surface* is required for useful shelter estimates.

For comparison with Seginer (1975), the protection distance for 50-cm height, where shelter speeds reached 80% of the approach windspeed, was near 4*H* in more oblique flow on the 10th, On the 13th, the value is close to 7*H*, providing the ratio 0.57, between the two protection distances. Note that the ratio changes with height, being closer to 7.2/8.6, or 0.84 at 2 m (z/Z~0.2). This is a likely cause of disagreement in plots of protection distance. Based on numerical simulations, Wang and Takle (1995) conclude that protection distance may be either larger or smaller than predicted by the cosine of the incidence angle, depending on combined effects of height, density, and width of shelter.

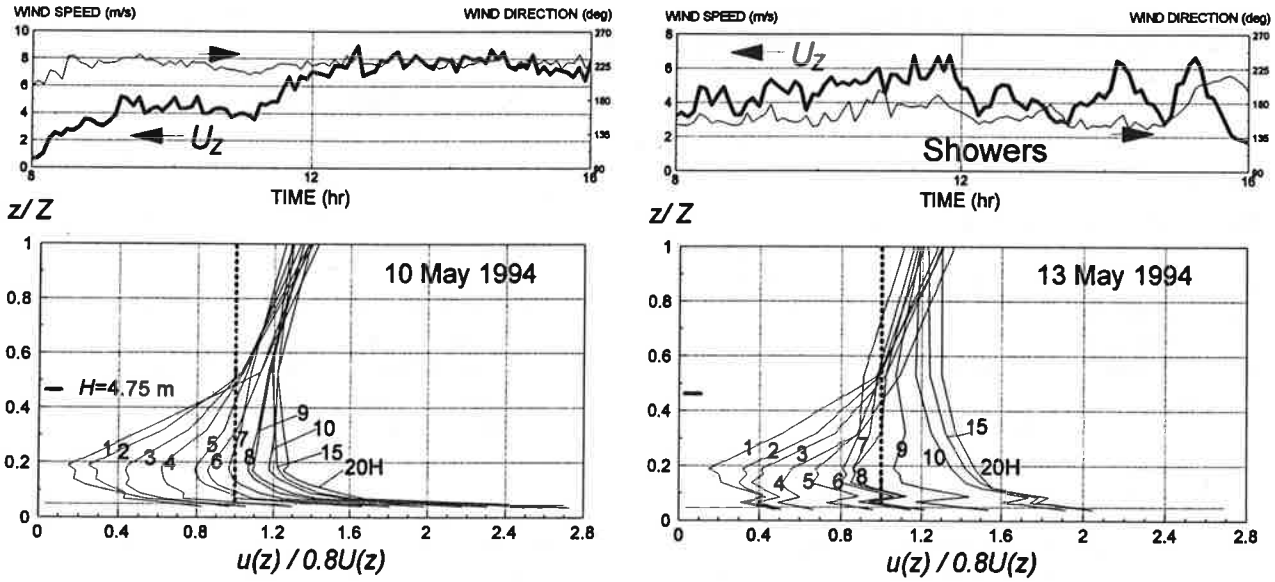

FIG. 7. Normalizing wind profiles in the lee of the redcedar windbreak, by 80% of the approach wind speed at the same height, maps shelter regions to the left of the dashed line. The number identifying each profile indicates downwind distance perpendicular to the barrier, in units of *H*. Reference height *Z* is 9.8 m at the top of the upwind mast, where U_Z is measured. Shelter for southwest flow on the 10th is less than for southerly flow on the 13th.

Static pressure at the surface increases approaching a barrier, shows a pressure drop through the barrier, and increases with downwind distance in the lee (Schmidt et al. 1995). In oblique flow, forces resulting from the gradients of static pressure turn flow near the fence, explaining the flow patterns observed by Mulhearn and Bradley (1977) for oblique fences in the wind tunnel. Numerical simulations (Wang and Takle, 1995, Fig. 2) predict that deviations from an oblique wind incidence angle increase with decreasing height, suggesting additional turbulent kinetic energy from the vertical shear of wind direction. Alkhalil et al. (1995) present a method of estimating windbreak drag under these conditions.

The effect of windbreak shelter on turbulent exchange in protected crop canopies is one link between aerodynamic models and estimates of economic benefits. With oblique flow, the lateral (cross-stream) turbulence component is likely to influence turbulent exchange substantially. Prueger et al. (1995) report energy balance studies made in concert with our mean vertical profile measurements.

5. CONCLUSION

Estimating benefits of shelterbelt networks on a landscape scale requires predicting windbreak shelter in oblique winds. The mobility of the instrumentation described in this paper, together with the capacity for real-time testing of hypotheses developed in our modeling effort, will speed improvements in understanding this complex flow, and the exchange processes that make it economically important.

Acknowledgements. Parts of this research were supported by USDA/CSRS Grant #93371018954. The National Institute for Global Environmental Change (DOE) supported additional parts of our work.

REFERENCES

Alkhalil, A., I. V. Litvina, E. S. Takle, R. A. Schmidt, and J. R. Brandle, 1995: Determination of drag properties of a shelterbelt from measurements and a numerical model. *Proc. 11th Symposium on Boundary Layers and Turbulence*, 27-31 March, Charlotte, NC. Amer. Meteor. Soc., Boston, MA.

Bernstein, A. B., 1966: A note on the use of cup anemometers in wind profile experiments. *J. Applied Meteor.* 6, 280-286.

Heisler, G. M., and D. R. DeWalle, 1988: Effects of windbreak structure on wind flow. *Agric. Ecosystems Environ.*, 22/23, 41-69.

Hetzler, R. E., W. O. Willis, and E. J. George, 1967: Cup anemometer behavior with respect to attack angle variation of the relative wind. *Trans ASAE 1967,* 376-377.

Jairell, R. L., R. D. Tabler, and R. A. Schmidt, 1984: Portable ten-meter instrument mast. *Proceedings, Western Snow Conference,* April, 1984, Sun Valley, ID. Colorado State University, 168-171.

McNaughton, K. G., 1988: Effects of windbreaks on turbulent transport and microclimate. *Agric. Ecosystems Environ.*, 22/23, 17-39.

Mulhearn, P. J., and E. F. Bradley, 1977: Secondary flows in the lee of porous shelterbelts. *Boundary-Layer Meteor.* 12, 75-92.

Prueger, J. H., T. J. Sauer, E. S. Takle, I. V. Litvina, R. A. Schmidt, J. R. Brandle, and J. L. Hatfield, 1995: Windbreak shelter effects on surface energy balance components. *Proc. 9th Symposium on Meteorological Observations and Instrumentation*, 27-31 March, Charlotte, NC. Amer. Meteor. Soc., Boston, MA.

Schmidt, R. A., E. S. Takle, J. R. Brandle, and I. V. Litvina, 1995: Static pressure at the ground under atmospheric flow across a windbreak. *Proc. 11th Symposium on Boundary Layers and Turbulence*, 27-31 March, Charlotte, NC. Amer. Meteor. Soc., Boston, MA.

Seginer, I., 1975. Flow around a windbreak in oblique wind. *Boundary-Layer Meteor.* 9, 133-141.

Tabler, R. D., 1980: Self-similarity of wind profiles in blowing snow allows outdoor modeling. *J. Glaciol.* 26, 421-434.

Taylor, Peter A., 1988: Turbulent wakes in the atmospheric boundary layer. *In*: Steffen, W. L. and O. T. Denmead (eds.) *Flow and Transport in the Natural Environment: Advances and Applications*, Proc. of an Int. Symp., Canberra, 1987. Springer-Verlag, New York, 270-292.

Wang, H. and E. S. Takle, 1995: Simulations of mean and turbulent properties of oblique flows near agricultural shelterbelts. *Proc. 11th Symposium on Boundary Layers and Turbulence*, 27-31 March, Charlotte, NC. Amer. Meteor. Soc., Boston, MA. (this volume).

Van Eimern, J., R. Karschon, L. A. Razumova, and G. W. Robertson, 1964: Windbreaks and Shelterbelts. WMO Technical Note No. 59 (WMO-No. 147.TP.70), 188 p.